

# Effect of Microenvironment on the Fluorescence of 2-Hydroxy-Substituted Nile Red Dye: A New Fluorescent Probe for the Study of Micelles

Krisztina Nagy, Sinem Göktürk,<sup>†</sup> and László Biczók\*

Chemical Research Center, Hungarian Academy of Sciences, P.O. Box 17, 1525 Budapest, Hungary

Received: May 16, 2003; In Final Form: July 29, 2003

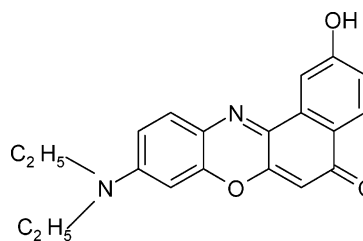
Absorption spectra and fluorescence properties of 2-hydroxy-substituted Nile Red (HONR) have been studied in various solvents and micelles. The solvent dependence of the rate constant of the internal conversion was found to exhibit two entirely distinct domains. Going from apolar toward polar solvents, first, the deceleration of the radiationless deactivation was observed due to the diminishing extent of the vibronic coupling between the neighboring  $S_1$  and  $S_2$  singlet excited states. After reaching a minimum, the rate of the transition to the ground state significantly increased in alcohols because of the efficient energy dissipation via intermolecular hydrogen bonding. The correlations of the excited-state energy, fluorescence lifetime, absorption, and fluorescence maxima with the  $E_T(30)$  solvent polarity parameter were used to characterize the local environment of HONR in micelles. Fluorescence quenching studies provided further evidences for the differences in the binding site of the dye in cationic, anionic and nonionic micelles.

## Introduction

The hydrophobic solvatochromic dye Nile Red has been a popular fluorescent probe in biological and medical research to localize and quantitate lipids,<sup>1</sup> to stain proteins,<sup>2</sup> and to detect ligand-binding to enzymes.<sup>3</sup> The remarkable sensitivity of its fluorescence characteristics was exploited in the design of luminescence-based sensors,<sup>4</sup> in probing of the supercages in zeolites,<sup>5</sup> in direct observation of solute distribution in chromatography,<sup>6</sup> and in the study of the accessibility of a hydrophobic surface in the photoactive yellow protein.<sup>7</sup> Fluorescence decay measurements revealed the relaxation dynamics of the excited dye in micelles<sup>8</sup> and the link between proton transport and water content in lipid membranes.<sup>9</sup>

Despite the widespread use of Nile Red, very few information is available on the photophysical properties of its substituted derivatives.<sup>10</sup> In the present work, we have explored how the introduction of a hydroxy group in the position 2 affects the fluorescent behavior, and demonstrated that the 2-hydroxy derivative of Nile Red (HONR) is an excellent probe for the study of micelles. The formula of HONR is presented in Scheme 1. The choice of compound was motivated by the following considerations. First, the hydroxy substitution is expected to decrease the solubility of the dye in alkanelike media, such as the micelle core, and it ensures its localization in the interfacial layer. On the other hand, the phenolic OH group can provide a binding site for hydrogen-bond acceptors and light absorption may enhance its acidity, leading to excited state proton transfer. Additional interest in HONR derives from the anticipation that the rate of the radiationless deactivation from its singlet-excited state depends strongly on the local environment. We have recently shown that the fluorescence lifetime of Nile Red markedly decreases with the increase of the hydrogen-bond donating ability in alcohols because vibrations associated with hydrogen-bonding are involved in the energy dissipation

## SCHEME 1



HONR

process.<sup>11</sup> As an extension of this study, now, we focus on HONR and unveil the major factors governing its fluorescent behavior in various solvents as well as in the aqueous solutions of cationic (CTAB), nonionic (TX-100), and anionic (SDS) surfactants. In addition, we elucidate the binding site and the polarity of the microenvironment of HONR in the micellar phase.

## Experimental Details

HONR, also called 9-diethylamino-2-hydroxy-5H-benz[a]-phenoxazin-5-one, and solvents (Aldrich, highest grade) were used without further purification; 1 M tetrabutylammonium hydroxide solution in methanol was purchased from Aldrich. The UV-visible absorption spectra were obtained with a Hewlett-Packard 8452 diode-array spectrophotometer. Corrected fluorescence and excitation spectra were recorded on a Jobin-Yvon Fluoromax-P photon counting spectrofluorometer. Fluorescence quantum yields were determined relative to that of cresyl violet in methanol, for which reference yield of 0.545 was taken.<sup>12</sup> Fluorescence lifetimes were measured with time-correlated single-photon counting technique. The light of a Picoquant diode laser (pulse duration 60 ps fwhm, wavelength 400 nm) excited the samples and the fluorescence decay was detected with a Hamamatsu H5783 photosensor module, which was connected to a Picoquant Timeharp 100 electronics (36 ps/

\* Corresponding author. E-mail: biczok@chemres.hu.

<sup>†</sup> Permanent address: Dean of Faculty of Pharmacy, Marmara University, Tibbiye cad. 81010, Kadikoy, Istanbul, Turkey.

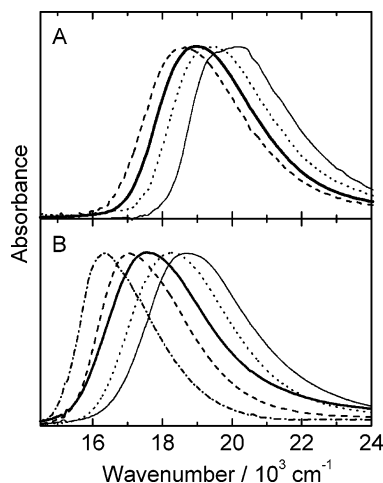


**Figure 1.** Absorption spectra of HONR: (A) in aprotic solvents dibutyl ether (—), ethyl acetate (···), acetone (— —), and propylene carbonate (- - -); (B) in alcohols decanol (—), methanol (···), ethylene glycol (— —), 1,1,1-trifluoroethanol (- - -), and 1,1,1,3,3,3-hexafluoro-2-propanol (— · — ·).

channel time resolution). Data were analyzed by a nonlinear least-squares deconvolution method using Picoquant FluoFit software. The quality of the fit was judged by the reduced  $\chi^2$  being close to unity and the random distribution of the weighted residual and autocorrelation values.

Sodium dodecyl sulfate (SDS, Fluka), cetyltrimethylammonium bromide (CTAB, Fluka), and Triton X-100 (TX-100, Aldrich) were used as received, because they were free from fluorescent impurities. Double distilled water was employed in the preparation of the micellar solutions. An appropriate amount of HONR/methanol stock solution was added to a flask and the methanol was evaporated by letting nitrogen flow over the solution. After adding the surfactant aqueous solution, the sample was stirred and left overnight for equilibration. Typical HONR concentration was  $8 \mu\text{M}$  and the lowering of the amount of the dye did not influence the results.

## Results and Discussion

**HONR in Organic Solvents.** In an effort to gain a better understanding of the factors controlling the relaxation of the excited HONR, we have studied systematically the solvent effect on the photophysical properties. As a representative example, Figure 1 displays the appreciable shift of the absorption spectra in various media. In the series of *n*-alkanols (Figure 1B) only a moderate change appears in the absorption spectra, but the interaction with fluorinated alcohols lowered substantially the energy of the first band because of the more pronounced hydrogen-bond donating character of the latter solvents.

Also the fluorescence spectra exhibit a remarkable solvent effect. (Figure 2) An increase in polarity induces not only a substantial red shift but also a marked modification in the shape of the emission band. The well-resolved vibrational progression, appearing in methylcyclohexane, gradually vanishes, and the half-width of the spectral band concomitantly decreases proceeding toward more polar solvents. The broader fluorescence band in apolar media may originate from the interaction with a close-lying  $S_2$  singlet excited state.

The energy of the lowest singlet excited state ( $E(S_1)$ ) was derived from the location of the intersection of the normalized absorption and fluorescence spectra. The results depicted in Figure 3A shows the decrease of  $E(S_1)$  as a function of the  $E_T(30)$  solvent polarity parameter.<sup>13</sup> The marked solvent effect

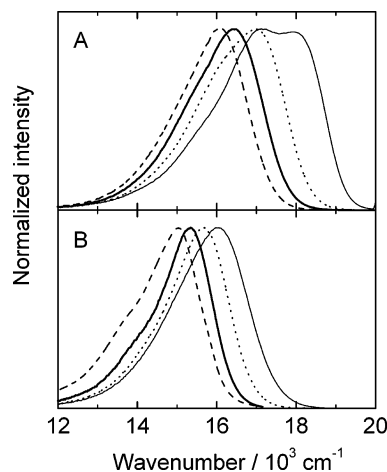


**Figure 2.** Fluorescence spectra of HONR: (A) in aprotic solvents dibutyl ether (—), ethyl acetate (···), acetone (— —), and propylene carbonate (- - -); (B) in alcohols decanol (—), methanol (···), 1,1,1-trifluoroethanol (— —), and 1,1,1,3,3,3-hexafluoro-2-propanol (- - -).

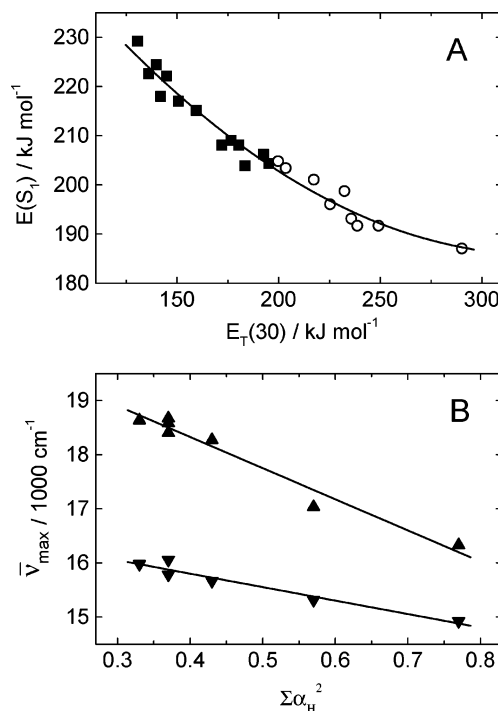


**Figure 3.** (A) Correlation between the energy of the lowest singlet excited state and the  $E_T(30)$  solvent polarity parameter in aprotic (■) and hydroxylic (○) solvents. (B) Absorption (▲) and fluorescence (▼) maxima plotted against the  $\Sigma\alpha_2^H$  hydrogen-bond acidity parameter.

implies that the lowest singlet excited state possesses charge transfer character because the conjugation of the lone electron pair of the diethylamino substituent raises the negative charge density on the carbonyl residue. Due to the high electron density of the carbonyl oxygen, this is probably the preferred site for hydrogen-bonding. The energies measured in both aprotic and hydroxylic solvents can be described with the same function, which will be utilized for the monitoring of the environment of HONR in micelles (vide infra).

It is worth noting that the absorption and fluorescence maxima diminish linearly with the growing hydrogen-bonding power of the solvents as measured by M. H. Abraham's  $\Sigma\alpha_2^H$  hydrogen-bond acidity parameter.<sup>14</sup> (Figure 3B) The Stokes shift is larger in alcohols of weaker hydrogen-bonding power as a result of the considerably higher hydrogen-bonding ability of

**TABLE 1: Photophysical Properties of HONR in Various Solvents**

solvent	$E_T(30)^a$ , kJ M <sup>-1</sup>	$\bar{\nu}_{\max}(\text{abs})$ , cm <sup>-1</sup>	$\bar{\nu}_{\max}(\text{fl})$ , cm <sup>-1</sup>	$E(S_1)$ , kJ M <sup>-1</sup>	$\tau_F$ , ns	$\Phi_F$	$k_F$ , 10 <sup>8</sup> s <sup>-1</sup>	$k_{IC}$ , 10 <sup>8</sup> s <sup>-1</sup>
cyclohexane	130.6	19450	18950	229.2	2.21	0.51	2.31	2.22
CCl <sub>4</sub>	136.1	19060	18130	222.6	3.74	0.70	1.87	0.80
dibutyl ether	139.8	19440	18030	224.4	3.56	0.66	1.86	0.95
toluene	141.9	19050	17610	218.0	3.82	0.76	2.00	0.62
diethyl ether	144.9	19650	17740	222.1	4.13	0.77	1.86	0.56
dioxane	150.7	19450	17270	217.0	4.07	0.78	1.92	0.54
ethyl acetate	159.5	19380	16990	215.1	4.33	0.79	1.82	0.48
CH <sub>2</sub> Cl <sub>2</sub>	172.1	18600	16600	208.1	4.42	0.81	1.83	0.43
acetone	176.7	18950	16450	209.0	4.55	0.78	1.72	0.48
butyronitrile	180.5	18870	16370	208.1	4.50	0.77	1.70	0.52
dimethylformamide	183.4	18560	16060	203.9	4.26	0.74	1.73	0.62
acetonitrile	192.6	18820	16210	206.2	4.50	0.74	1.64	0.59
propylene carbonate	195.1	18600	16100	204.3	4.42	0.70	1.58	0.68
1-decanol	199.7	18670	16060	204.8	4.01	0.60	1.50	1.00
2-propanol	203.5	18640	15980	203.4	4.01	0.59	1.48	1.01
1-pentanol	205.6	18500	15900	204.0	4.00	0.58	1.45	1.05
1-butanol	210.2	18450	15860	203.0	3.98	0.57	1.43	1.08
1-propanol	212.3	18580	15810	202.0	3.97	0.57	1.44	1.08
ethanol	217.3	18400	15780	201.1	3.79	0.58	1.54	1.10
diethylene glycol	225.2	17860	15530	196.0	3.43	0.61	1.78	1.14
CH <sub>3</sub> OH	232.4	18270	15660	198.7	3.08	0.47	1.54	1.71
CH <sub>3</sub> OD	232.4	18240	15660	198.7	4.0	0.70	1.76	0.74
1,2-ethanediol	235.7	17540	15350	193.1	2.83	0.41	1.45	2.08
glycerol	238.6	17110	15270	191.7	2.69	0.40	1.49	2.23
CF <sub>3</sub> CH <sub>2</sub> OH	249.1	17030	15310	191.7	2.06	0.24	1.17	3.68
(CF <sub>3</sub> ) <sub>2</sub> CHOH	290.1	16330	14920	187.1	0.95	0.087	0.91	9.61

<sup>a</sup> Reference 13.

the excited state. Fluorinated alcohols are complexed with HONR already in the ground state. Hence, the extent of solvent shell reorganization upon excitation is smaller in these media.

Table 1 gives an extensive list of the photophysical parameters. From the solvent dependence of the Stokes shift ( $\bar{\nu}_{\max}(\text{abs}) - \bar{\nu}_{\max}(\text{fl})$ ), the difference of the dipole moments in the excited ( $\mu_e$ ) and ground ( $\mu_g$ ) states can be derived based on the Lippert–Mataga equation

$$\bar{\nu}_{\max}(\text{abs}) - \bar{\nu}_{\max}(\text{fl}) = \frac{2(\mu_e - \mu_g)^2}{hca^3} F1 + C1 \quad (1)$$

where F1 refers to the polarity parameter  $F1 = [(\epsilon - 1)/(2\epsilon + 1)] - [(n^2 - 1)/(2n^2 + 1)]$ ;  $c$ ,  $h$ ,  $\epsilon$ , and  $n$  denote the speed of light, Planck constant, dielectric constant, and refractive index of the medium, respectively;  $a$  is the radius of the cavity surrounding the dye, and C1 is a constant. Figure 4A shows the Stokes shift plotted against the F1 solvent parameter. Since eq 1 is valid for dielectric solvent–solite interactions, the data obtained in strongly hydrogen-bonding solvents are not included. A good linear correlation appears and from the slope,  $\mu_e - \mu_g = 8.9$  D is calculated taking  $a = 0.5$  nm, the value usually used for Nile Red.<sup>15</sup>

Periasamy and co-workers have recently pointed out that the ratio of the dipole moments for the excited and the ground-state molecules ( $\mu_e/\mu_g$ ) can be calculated without assuming any value for the cavity radius of the dye.<sup>16</sup> Plotting the sum of the absorption and the fluorescence maxima in the function of  $F2 = [(\epsilon - 1)/(2\epsilon + 1)] - [(n^2 - 1)/(2n^2 + 1)]$  gives a linear relationship (Figure 4B), which is described by

$$\bar{\nu}_{\max}(\text{abs}) + \bar{\nu}_{\max}(\text{fl}) = -\frac{2(\mu_e^2 - \mu_g^2)}{hca^3} F2 + C2 \quad (2)$$

where C2 is a constant. From the combined analysis of the slopes obtained from Figure 4, parts A and B,  $\mu_e/\mu_g = 2.6$  is calculated in agreement with the significant charge-transfer

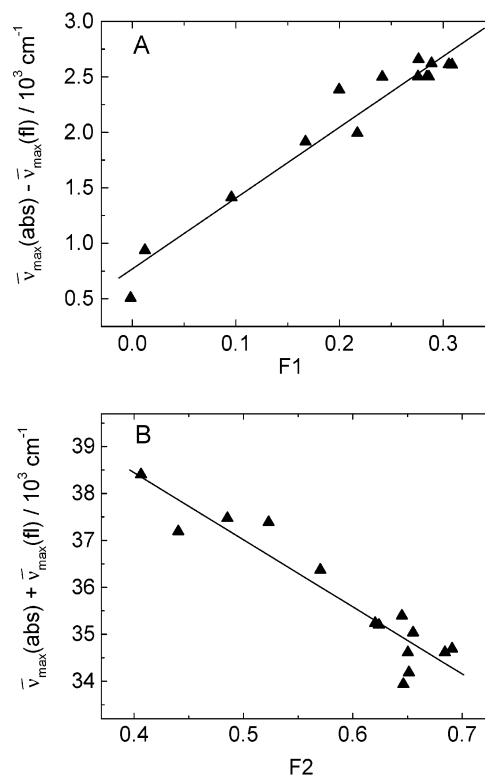


**Figure 4.** Determination of the dipole moment enhancement upon excitation (A) based on the Lippert–Mataga equation and (B) plot of the data according to eq 2.

character of the excited HONR. The  $\mu_e - \mu_g = 8.9$  D and  $\mu_e/\mu_g = 2.6$  values, derived based on eqs 1 and 2, provide  $\mu_e = 14.5$  D and  $\mu_g = 5.6$  D for the dipole moment of the excited and ground-state HONR, respectively.

The insert to Figure 5 clearly shows that the absorption spectrum of HONR broadens and the maximum shifts from 18270 to 19100 cm<sup>-1</sup> on addition of 9.9 mM tetrabutylammonium hydroxide (Bu<sub>4</sub>NOH) in methanol. These changes are

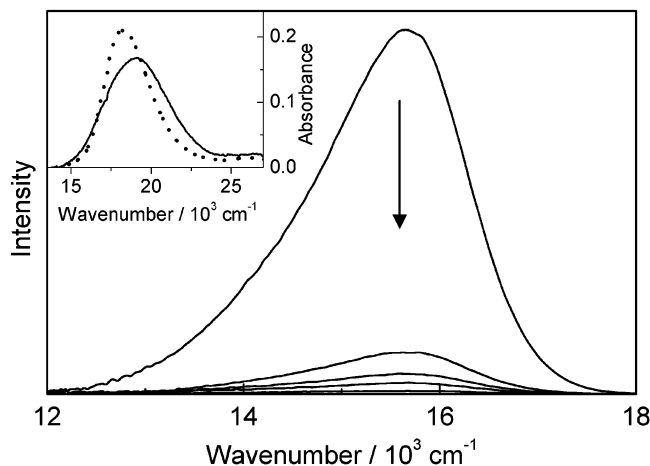


**Figure 5.** Alteration of fluorescence spectra on addition of 0, 0.33, 0.67, 1.33, and 6.3 mM tetrabutylammonium hydroxide in methanol (excitation at  $19300\text{ cm}^{-1}$ ). Inset: absorption spectra in the presence of 0 mM (dotted line) and 9.9 mM (solid line) tetrabutylammonium hydroxide in methanol.

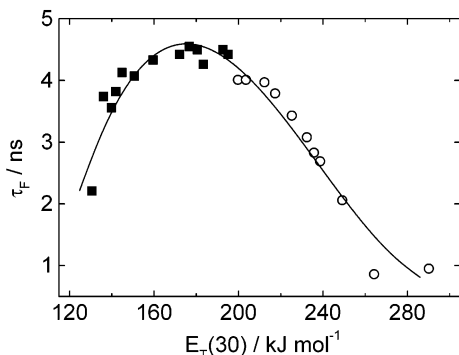


**Figure 6.** Change of the fluorescence lifetime as a function of  $E_T(30)$  solvent polarity parameter.

assigned to the deprotonation of the phenolic OH group in the presence of base, and the solid line represents the spectrum of the phenolate anion form of HONR. Figure 5 also demonstrates the more than 2 orders of magnitude decrease of the fluorescence intensity, when the  $\text{Bu}_4\text{NOH}$  concentration is raised from 0 to 9.9 mM, indicating that the phenolate anion form of HONR barely fluoresces. Similar results were achieved using NaOH as base in 5% methanol aqueous solutions.

In neat organic solvents the deprotonation of the phenolic HO group in the excited state can be excluded based on the following facts. The photophysical properties of HONR proved to be very similar to those of the unsubstituted Nile Red.<sup>11</sup> The fluorescence decays were strictly single exponential in all solvents: the reduced  $\chi^2$  values were always within the 1.00–1.20 range; both the weighted residual and the autocorrelation values showed random distribution. The only exception was the highly viscous glycerol, in which the slow solvation dynamics caused dual exponential decay at the high and the low energy edge of the HONR fluorescence band. In the other solvents, the fluorescence lifetimes were independent of the emission wavelength because the solvation dynamics were faster than the time-resolution of our instrument.

It is evident from the data in Table 1 that the fluorescence lifetime ( $\tau_F$ ) changes parallel with the fluorescence quantum yield ( $\Phi_F$ ) and both quantities go through a maximum with increasing solvent polarity. As the accuracy of  $\tau_F$  is better, we present its solvent dependence in Figure 6. Two entirely distinct regions can be seen, indicating the alteration of the deactivation

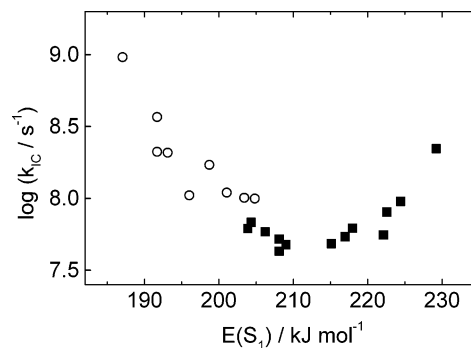


**Figure 7.** Logarithm of the internal conversion rate constant plotted against the energy of the lowest singlet excited state in aprotic (■) and hydroxylic (○) solvents.

mechanism of the singlet excited HONR. After the gradual initial increase,  $\tau_F$  tends to level off in solvents of medium polarity and then diminishes in alcohols. To reveal the dominant factors of the energy dissipation, the rate constants for fluorescence emission ( $k_F$ ) and internal conversion ( $k_{IC}$ ) are derived using the expressions given below:

$$k_F = \Phi_F / \tau_F \quad (3)$$

$$k_{IC} = (1 - \Phi_F) / \tau_F \quad (4)$$

These equations are valid because neither photochemical reaction nor transition to the triplet-excited state can be detected. Excitation of the deoxygenated HONR solutions with the 532 nm light of a Nd:YAG laser (Continuum Surelight, pulse width at half-maximum 6 ns, energy 30 mJ) produced neither transient absorption nor bleaching.

The results compiled in Table 1 demonstrate that the internal conversion rate constant controls the solvent dependence of the fluorescence lifetime; the change of the radiative rate constant is much smaller. The diminution of  $k_F$  proceeding toward polar solvents can be rationalized in terms of the Strickler–Berg equation<sup>17</sup>

$$k_F = 2.88 \times 10^{-9} n^2 (\bar{\nu}^{-3})_{av}^{-1} \int \epsilon d(\ln \bar{\nu}) \quad (5)$$

where  $n$  is the refractive index of the solvent,  $(\bar{\nu}^{-3})_{av}^{-1}$  denotes an average over the fluorescence spectrum, and the integral extends over the first absorption band. This relationship predicts that the radiative rate constant decreases approximately as the cube of the emission energy. Therefore, a smaller  $k_F$  is expected and found, indeed, in polar solvents because of the red shift of the fluorescence spectrum.

The rate constant of the internal conversion exhibits an entirely different trend. Figure 7 presents the plot of the logarithm of  $k_{IC}$  against the energy of the lowest excited singlet state ( $E(S_1)$ ) in various solvents. Two readily distinguishable ranges appear: going from methylcyclohexane to ethyl acetate the internal conversion slows down, whereas in more polar solvents marked rate enhancement is observed. It is well-established that vibronic coupling between close-lying singlet excited states leads to very efficient radiationless relaxation.<sup>18</sup> This phenomenon seems to be responsible for the rapid internal conversion in nonpolar media. Our results suggest that in methylcyclohexane the  $S_2$  excited state is located very close in energy to the  $S_1$  state. As the polarity of the medium grows, the solvent–solute interactions stabilize the excited state of charge-transfer character much more than the other state, which has a smaller dipole moment. Consequently, the  $S_1 - S_2$  energy gap is expanded in more polar solvents and the less effective

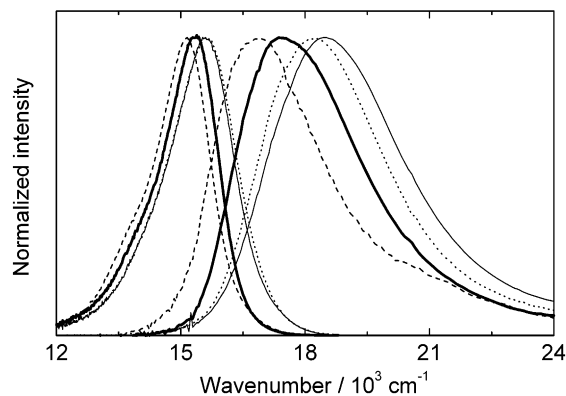


**Figure 8.** Absorption and fluorescence spectra of HONR in 0.02 M SDS (—), CTAB (---), TX100 (···) solutions and in water (- - -).

vibrational coupling between the adjacent states decelerates internal conversion. The extent of the  $k_{IC}$  decrease is smaller than reported previously for aromatic ketones and nitrogen heterocyclic compounds.<sup>18</sup> This may indicate that for HONR neither of the vibronic coupled states are of  $n\pi^*$  character. In moderately polar solvents, such as  $\text{CH}_2\text{Cl}_2$  and acetone,  $S_2$  state is situated well above the  $S_1$  state, which precludes their interaction. Further increase of the solvent polarity results in considerable lessening of  $E(S_1)$  and intensifies the vibrational coupling with the ground state leading to substantial increase in  $k_{IC}$ , as it is expected based on the energy gap law.<sup>19</sup>

It is noteworthy that both the fluorescence yield and the fluorescence lifetime are considerably larger in  $\text{CH}_3\text{OD}$  compared with the corresponding values in  $\text{CH}_3\text{OH}$  (Table 1). The significant isotope effect indicates that hydrogen bonding provides an effective accepting mode for dissipation of excitation energy. A similar conclusion has been drawn for the unsubstituted Nile Red dye.<sup>11</sup>

**HONR in Micelles.** On the basis of its characteristic responses to different solvents, HONR can serve as a sensitive probe of micelles. The solubility of the dye in aqueous surfactant solutions increases considerably above the critical micelle concentration and a hypsochromic shift of both the absorption and the fluorescence spectra can be observed. In 0.02 M, surfactant solutions the solubilization of the dye in the micelles is practically complete because further addition of surfactants failed to bring about any spectral change. Figure 8 presents the spectra in micelles and, for the sake of comparison, also in water.

The spectra do not resemble the structured band obtained in neat apolar solvents indicating that HONR is not included in the alkanelike micellar core. The marked blue shift of the peak compared with that in water is consistent with the dye being confined close to the interfacial layer of the micelles. Time-resolved fluorescence measurements also support this conclusion. The fluorescence decays, detected at 700 nm, fit well to a single-exponential function, and the fluorescence lifetimes are given in Table 2 together with the other parameters of HONR incorporated in the micellar phase. In SDS micelle,  $\tau_F$  proved to be shorter than in CTAB and TX-100 micelles, but all  $\tau_F$  values are significantly larger than in water.

**TABLE 2: Photophysical Parameters of HONR in 0.02 M Surfactant Solutions and the Polarity of the Microenvironment around the Dye in Micelles**

media	$\bar{\nu}_{\max}(\text{abs})$ , $\text{cm}^{-1}$	$\bar{\nu}_{\max}(\text{fl})$ , $\text{cm}^{-1}$	$E(S_1)$ , $\text{kJ M}^{-1}$	$\tau_F$ , ns	$E_T(30)$ in micelles, $\text{kJ M}^{-1}$			
					from $\bar{\nu}_{\max}(\text{abs})$	from $\bar{\nu}_{\max}(\text{fl})$	from $E(S_1)$	from $\tau_F$
TX	18160	15630	198.6	3.37	218	223	219	225
CTAB	18440	15630	198.3	3.18	205	223	220	229
SDS	17460	15360	192.4	2.42	246	247	248	248
water	16900	15140	188.3	0.86				

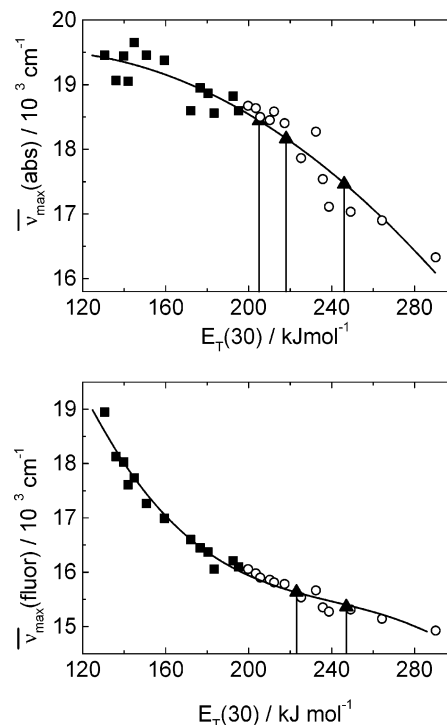


**Figure 9.** Change of the absorption (A) and fluorescence (B) maxima with increasing  $E_T(30)$  solvent polarity parameter in aprotic (■) and hydroxylic (○) solvents. (▲) Derivation of the  $E_T(30)$  for micelles. The obtained values are given in Table 2.

To assess the subtle differences in the microenvironment, the excited-state energy (Figure 3A), fluorescence lifetime (Figure 6), and absorption and fluorescence maxima (Figure 9) measured in neat solvents are plotted against the  $E_T(30)$  polarity parameter and the data are fitted with a polynomial. These calibrations are used to characterize the surroundings around the dye in the self-assembled surfactant aggregates and Table 2 summarizes the  $E_T(30)$  values of the microenvironment in micelles determined by the four different methods. HONR senses significantly higher polarity for SDS micelle owing to the greater water accessibility. This is in accord with the previous findings that micelles with anionic headgroups are more hydrated than their cationic counterpart.<sup>20,21</sup> The local environment around the probe is very similar in CTAB and TX-100 and resembles the polarity of diethylene glycol, whereas in SDS micelle that is close to the polarity of trifluoroethanol. The analogous surroundings of HONR in CTAB and TX-100 indicate the negligible contribution of the ionic charges to the local polarity.

As it is seen in Table 2, the  $E_T(30)$  values derived from the different type of measurements agree well for each micelle. The only exception is the polarity parameter stemming from the absorption maximum in CTAB. This is somewhat lower than the corresponding results based on the fluorescence lifetime and the fluorescence maximum. However, such a deviation is not found for SDS and TX-100. For the latter micelles the width of the absorption band at the half-maximum is  $3500 \text{ cm}^{-1}$ , contrary to the value of  $3800 \text{ cm}^{-1}$  obtained for CTAB. The

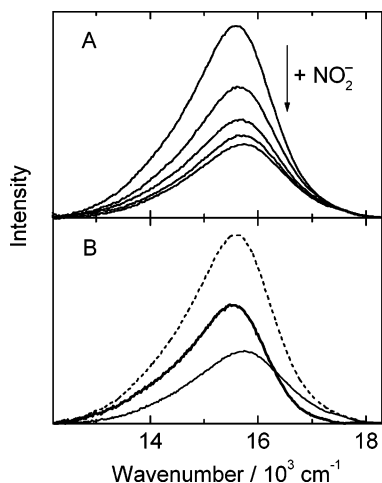


**Figure 10.** (A) Fluorescence quenching of  $8 \mu\text{M}$  HONR confined in CTAB micelle,  $[\text{CTAB}] = 0.02 \text{ M}$ , with increasing  $\text{NaNO}_2$  concentration: 0, 0.95, 2.2, 3.7, 100 mM; excitation wavelength: 530 nm. (B) Resolution of the fluorescence spectrum: spectrum in the absence of  $\text{NaNO}_2$  (---), spectra for HONR in the Stern layer (—), and the fluorescence in the presence of 0.1 M  $\text{NaNO}_2$  (- -).

broader absorption peak may imply that HONR occupies distinct binding sites.

To confirm this conception, fluorescence quenching experiments have been carried out. Because of its low oxidation potential (1.04 V vs NHE),  $\text{NO}_2^-$  anion readily donates electron to excited dyes leading to quenching via electron-transfer process.<sup>22</sup> Figure 10A displays the change of the fluorescence spectrum for CTAB micelle with increasing  $\text{NaNO}_2$  concentration. It is seen that the diminution of the fluorescence intensity is accompanied by the blue shift of the maximum in the 0–0.1 M  $\text{NaNO}_2$  concentration range, but the spectral band remains unchanged with further addition of the salt. Addition of  $\text{NaCl}$ , the compound which is unable to react with HONR in electron-transfer process because of its unfavorable redox potential, does not cause such spectral alteration that was observed in the presence of  $\text{NaNO}_2$ . Thus, the changes presented in Figure 10 cannot arise from the mere salt effect on the micelle structure. This provides further support to the claim that HONR resides in two distinct regions within the CTAB micelle. Since emission from the bulk aqueous phase is precluded based on the low solubility and fluorescence yield of HONR in water, the fluorescence component sensitive to  $\text{NO}_2^-$  is assigned to the dye molecules located in the Stern layer. The spectrum emitted by these species can be obtained as a difference of the fluorescence measured in the absence of additive and at 0.1 M  $\text{NaNO}_2$  concentration. (Figure 10B) The  $\text{NO}_2^-$  ions compete with  $\text{Br}^-$  for the cationic binding sites and become incorporated in the Stern layer. The close proximity of  $\text{NO}_2^-$  to the dye, located also in the interfacial layer, permits rapid quenching.

Because a fraction of the fluorescence cannot be quenched even at high  $\text{NO}_2^-$  concentration, we conclude that HONR resides not only in the Stern layer but also in the outer region of the micellar core, which cannot be reached by the quencher ions. The merely ca.  $220 \text{ cm}^{-1}$  hypsochromic displacement of the fluorescence maximum of these species with respect to the fluorescence peak of the probe located in the Stern layer implies that HONR inaccessible to the quencher is not deeply included in the micelle but solubilized close to the interface.

It is worth noting that  $\text{NO}_2^-$  fails to quench the fluorescence when HONR is incorporated in the SDS micelle. The repulsive electrostatic field due to the negative charge of the SDS micellar surface effectively retards the diffusional arrival of the anion

in the Stern layer. Consequently, in the anionic micelle, HONR is protected from quenching. However, when 0.1 M  $\text{Fe}^{2+}$  was added, 90% of the fluorescence was quenched. Since the most of the dye molecules stay in the Stern layer of the SDS micelle, the quencher cation can easily approach them. In contrast, neither  $\text{NO}_2^-$  nor  $\text{Fe}^{2+}$  affect the fluorescence when HONR is incorporated in the nonionic TX-100 micelle. This fact clearly shows the deeper inclusion of the dye in the polyoxyethylene mantle.

## Conclusion

The substitution of Nile Red in position 2 scarcely affects the photophysical properties but modifies the solubility, which can be advantageous in many applications. The solvent effect on the rate constant of the internal conversion is found to control the fluorescent behavior. The extent of the vibronic interaction between the two lowest singlet excited states is suggested to govern the rate of the radiationless deactivation in apolar solvents, whereas the hydrogen-bonding with alcohols and the decrease of the energy gap between the singlet excited and ground states significantly accelerate the energy dissipation in polar media. The marked solvent dependence of the fluorescence lifetime, the energy of the lowest singlet excited state as well as the absorption and fluorescence maxima can be utilized for the study of the local environment of HONR in microheterogeneous systems. The differences in the local polarity around the dye reflect the degree of the water accessibility of the binding site in various micelles. Fluorescence quenching experiments also support that the dye resides in the Stern layer for SDS micelle, deeper included in the palisade layer for TX-100 micelle and two binding sites exist in CTAB micelle.

**Acknowledgment.** The authors very much appreciate the support of this work by the Hungarian Scientific Research Fund (OTKA, Grant T034990), the 1/047 NKFP Medicchem Project and the Hungarian Academy of Sciences—TUBITAK scientific exchange program.

## References and Notes

- (1) (a) Al-Saffar, N. M. S.; Titley, J. C.; Robertson, D.; Clarke, P. A.; Jackson, L. E.; Leach, M. O.; Ronen, S. M. *Br. J. Cancer* **2002**, *86*, 963. (b) Morjani, H.; Aouali, N.; Belhoussine, R.; Veldman, R. J.; Levade, T.; Manfait, M. *Int. J. Cancer* **2001**, *94*, 157. (c) Klinkner, A. M.; Bugelski, P. J.; Waites, C. R.; Loudon, C.; Hart, T. K.; Kerns, W. D. *J. Histochem. Cytochem.* **1997**, *45*, 743.
- (2) (a) Sackett, D. L.; Wolff, J. *Anal. Biochem.* **1987**, *167*, 228. (b) Daban, J. R. *Electrophoresis* **2001**, *22*, 874. (c) Alba, F. J.; Bermudez, A.; Daban, J. R. *Electrophoresis* **2001**, *22*, 399. (d) Alba, F. J.; Bermudez, A.; Bartolome, S.; Daban, J. R. *Biotechniques* **1996**, *21*, 625.
- (3) Ruvinov, S. B.; Yang, X. J.; Parris, K. D.; Banik, U.; Ahmed, S. A.; Miles, E. W.; Sackett, D. L. *J. Biol. Chem.* **1995**, *270*, 6357.
- (4) (a) Levitsky, I. A.; Krivoslykov, S. G.; Grate, J. W. *J. Phys. Chem. B* **2001**, *105*, 8468. (b) Levitsky, I. A.; Krivoslykov, S. G.; Grate, J. W. *J. Phys. Chem. B* **2001**, *105*, 8468.
- (5) Uppili, S.; Thomas, K. J.; Crompton, E. M.; Ramamurthy, V. *Langmuir* **2000**, *16*, 265.
- (6) Lowry, M.; He, Y.; Geng, L. *Anal. Chem.* **2002**, *74*, 1811.
- (7) Hendriks, J.; Gensch, T.; Hviid, L.; van der Horst, M. A.; Hellingwerf, K. J.; van Thor, J. *J. Biophys. J.* **2002**, *82*, 1632.
- (8) (a) Datta, A.; Mandal, D.; Pal, S. K.; Bhattacharyya, K. *J. Phys. Chem. B* **1997**, *101*, 10221. (b) Krishna, M. M. G. *J. Phys. Chem. A* **1999**, *103*, 3589. (c) Maiti, N. C.; Krishna, M. M. G.; Britto, P. J.; Periasamy, N. *J. Phys. Chem. B* **1997**, *101*, 11051.
- (9) Krishnamoorthy, I.; Krishnamoorthy, G. *J. Phys. Chem. B* **2001**, *105*, 1484.
- (10) (a) Briggs, M. S. J.; Bruce, I.; Miller, J. N.; Moody, C. J.; Simmonds, A. C.; Swann, E. *J. Chem. Soc., Perkin Trans. 1* **1997**, 1051. (b) Long, J.; Wang, Y.; Matsuura, T.; Meng, J. *J. Heterocycl. Chem.* **1999**, *36*, 895.
- (11) Cser, A.; Nagy, K.; Biczók, L. *Chem. Phys. Lett.* **2002**, *360*, 473.
- (12) Magde, D.; Brannon, J. H.; Cremers, T. L.; Olmsted, J., III. *J. Phys. Chem.* **1979**, *83*, 696.
- (13) Reichardt, C. *Angew. Chem., Int. Ed. Engl.* **1979**, *18*, 98.

- (14) Abraham, M. H. *Chem. Soc. Rev.* **1993**, 73.
- (15) (a) Sakar, N.; Das, K.; Nath, D. N.; Bhattacharyya, K. *Langmuir*, **1994**, *10*, 326. (b) Dutta, A. K.; Kamada, K.; Ohta, K. *J. Photochem. Photobiol. A: Chemistry* **1996**, *93*, 57. (c) Golini, C. M.; Williams, B. W.; Foresman, J. B. *J. Fluoresc.* **1998**, *8*, 395.
- (16) Koti, A. S. R.; Bhattacharjee, B.; Haram, N. S.; Das, R.; Periasamy, N.; Sonawane, N. D.; Rangnekar, D. W. *J. Photochem. Photobiol. A: Chem.* **2000**, *137*, 115.
- (17) Strickler, S. J., Berg, R. A., *J. Chem. Phys.* **1962**, *37*, 814.
- (18) (a) Lim, E. C. *J. Phys. Chem.* **1986**, *90*, 6770. (b) Lim, E. C. *Excited States*; Academic: New York, 1977; Vol. 3, p 305.
- (19) (a) R. Englman, J. Jortner, *Mol. Phys.*, **18**, 1970 145. (b) K. F. Freed, J. Jortner, *J. Chem. Phys.* **1970**, *52*, 6272.
- (20) Karukstis, K. K.; Suljak, S. W.; Waller, P. J.; Whiles, J. A.; Thompson, E. H. Z. *J. Phys. Chem.* **1996**, *100*, 11125.
- (21) Bales, B. L.; Zana, R. *J. Phys. Chem. B* **2002**, *106*, 1926.
- (22) Loeff, I.; Rabani, J.; Treinin, A.; Linschitz, H. *J. Am. Chem. Soc.* **1993**, *115*, 8933.